Recent Advances in Rare Earth Doped Inorganic Crystalline Materials for Quantum Information Processing

Nathalie Kunkel [a] and Philippe Goldner [b]

Dedicated to Prof. Wolfgang Schnick on the Occasion of his 60th Birthday

[a] Dr. Nathalie Kunkel,
Chair for Inorganic Chemistry with Focus on Novel Materials, Department of Chemistry
Technical University of Munich
Lichtenbergstr. 4, 85747 Garching, Germany
E-mail: nathalie.kunkel@lrz.tu-muenchen.de
[b] Dr. Philippe Goldner
Institut de Recherche de Chimie Paris
PSL Research University, Chimie ParisTech, CNRS
11 rue Pierre et Marie Curie, 75005 Paris, France
Email : philippe.goldner@chimie-paristech.fr

Abstract: Since quantum information technologies are expected to offer communication security and high computational capacities, research in the field is currently attracting a lot of attention. Among the materials studied so far, rare earth doped inorganic insulators are one of the most promising. With the different available trivalent rare earth ions, the visible and the IR range including the telecom wavelength at 1.5 µm can be covered. Transitions are usually narrow, and at low temperatures, long optical and spin coherence time can often be observed. Investigations using bulk single crystals have already led to many promising results. Recently, spectroscopic studies have been extended to other forms of inorganic materials, such as transparent ceramics, thin films and nanoparticles for single rare-earth qubits. Progress in these areas is expected to offer many new possibilities for the design of quantum light-matter interfaces and scalable quantum memories and processors.

1. Introduction

Rare earth doped inorganic materials are well known for applications such as solid-state lighting, screens, lasers, scintillators, afterglow materials or sensors [1-4]. Advances in these fields required the development of suited materials, and understanding the relations between chemical, structural and optical properties. A well-known example are the rare earth doped compounds, which are nowadays widely used in the field of
white-light emitting diodes [5-6]. Initially, Schnick and co-workers [7-11] discovered the chemically and thermally stable Eu2+-doped nitridosilicates and oxonitridosilicates. This discovery then led to great improvements in the multiphosphor approach [12] for generating white light. And in spite of the progress already made, further efforts are made to find new narrow-band-emitting red phosphors [13], but also further phosphors for special applications such as horticultural lighting [14].
Many of such kind of developments are possible due to contributions of inorganic and materials chemists and their close collaborations to researchers in optical spectroscopy.
In another field of applications for rare earth doped inorganic materials - quantum information processing (QIP) – it is also expected that progress in the development of tailor-made materials will lead to great improvements. In the beginning of the technology, optical studies were often limited to the available single crystalline materials and commercial optical fibers. With the rapidly increasing need for quantum technologies, for example for secure communication, important progress on measurement techniques was made. Yet, the

development of these techniques critically depends on the type and quality of the available materials. As we shall explain later, prerequisites are for example a combination of long optical and spin coherences times, which requires the control of spectral diffusion or the possibility to control inhomogeneous and homogeneous line broadening. Thus, there is a need to develop materials beyond single crystals and to understand and control spectral diffusion in these materials in order to overcome the significant limitations and the lack of suited materials.

Only recently the importance of material design beyond single crystals growth has been fully recognized and in the last recent years, promising advances in the field of rare earth doped ceramics, films and (nano) powders especially designed for quantum technologies have been made. In the present research report, we therefore summarize some of the recent developments in materials design and emphasize the importance of further research on materials in order to develop sophisticated quantum devices, as for example single ion devices. Especially, we aim at elaborating the special requirements that spectroscopists and materials chemists are confronted with while developing such materials. Thus, we will not offer a profound and detailed review on the different spectroscopic techniques used in quantum technology and related fields. A number of detailed and interesting works on the topic is already available to the interested reader, such as for instance Ref. [15-18]. Review articles are also available, especially on the progress in the field on rare earth doped single crystals, for example Ref. [18-22]. Instead, we mainly summarize the advances already made in the design of non-single-crystalline materials in the field as well as very recent developments using single crystals. The present research report is organized as follows: In chapter (2) we introduce basic concepts and techniques for quantum information technology using rare earth ions and the related materials requirements. In chapter (3), we shall report on the recent progress made in polycrystalline materials for quantum technologies and also briefly review some recent developments related to rare earth doped single crystals and waveguides.

2. Quantum Information Technologies and Related Techniques

Information in digital form and optical data storage play an important role, both for large scale organizations down to our daily lives. In recent years, there has been a growing interest in quantum information processing, storage and communication [15-17, 22-27]. These applications offer both unprecedented computational capacities as well as nearly unconditional communication security via quantum cryptography. Achieving them in the solid state is particularly appealing for further technological developments.

2.1. Qubits

Equivalent to the bit in classical computing, the quantum bit (qubit) is the elementary unit of information. In contrast to the classical bit, which can take the two values 0 and 1, a qubit is a quantum two-level system. Its eigenstates $|0\rangle$ and $|1\rangle$ correspond to the classical binary values 0 and 1 (see Fig.1). Yet while the classical bit can only represent 0 or 1, the qubit can also adopt an arbitrary superposition state. This superposition state can be written in the following form [15]:

$$|\Psi\rangle = \cos(\theta/2)|0\rangle + e^{i\delta}\sin(\theta/2)|1\rangle \quad \text{(equ.1)}$$

|Ψ> and eiδ |Ψ> are equivalent wavefunctions and $e^{i\delta}$ a global phase factor. The fact that a qubit can adopt such an arbitrary superposition state allows to process and transmit data in ways that are unachievable with classical systems.

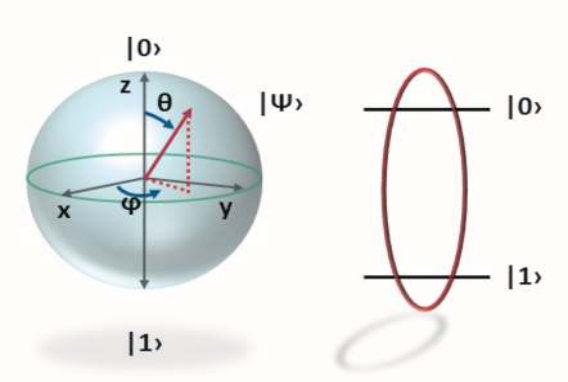

Figure 1. A qubit in a superposition state |Ψ>. Left: representation on the Bloch sphere. Right: superposition represented as ellipse.

To visualize superposition states, a convenient way is the use of vectors originating at the center of a Bloch sphere. The angles θ and φ from equation 1 are used to express the spherical coordinates of the vector on the sphere. The system adopts the states |0> and |1> when the vector points at the north, or the south pole, respectively. As a result, a qubit can adopt an infinite number of different states, but the only states, which can be identified with certainty are |0> and |1>.

To obtain reliable data transmission and calculation results, it is necessary to use superposition states, but also to be able to read out the final states with high probability. Additionally, superposition states are highly sensitive towards perturbations, so that isolated systems would be ideal. However, control and read out of the superposition states requires interactions with the environment. A number of suitable quantum systems are investigated, such as photons and nuclear spins in insulators and semiconductors, trapped ions, ultra-cold atoms and superconducting circuits [16-18, 28-35]. When light is used as a carrier of quantum information, it is necessary to interface it to materials in order to store and process information [36]. Furthermore, suitable lasers for efficient control and long-lived superposition states are a prerequisite. The lifetime of the superposition states and therefore the time available for quantum manipulation or storage is correlated to the so-called coherence time (T2), which shall be explained in the next section (chapter 2.2). The coherence properties critically depend on the type of material. One of the most promising materials classes among those studied so far are rare earth ions doped into dielectric host lattices [15, 22, 37]. Using transitions of rare earth ions, it is possible to cover the whole visible range as well the IR, as for example the telecom wavelength at 1.5 µm. At low temperature, these systems offer long optical and spin coherence states [15, 18, 22]. Line broadening can also be controlled by carefully adjusting the compositions and using interactions with external electric and magnetic fields [15, 18,22].

2.2. Inhomogeneous and homogeneous linewidths, coherence

The reason why the trivalent rare earth ions are such promising systems for quantum information applications is that their partially filled 4f shell is well shielded from the outer environment by the filled 5s2 and 5p6 shells and therefore, the 4fn-4fn transitions are only weakly perturbed by the crystalline environment. The 4f shell is so well-shielded that the crystal field can be considered as a weak perturbation of the free ion levels. Furthermore, the excited state lifetimes can be long lived, for example up to several ms. As a consequence, trivalent rare earth ions can show resonances that exhibit extremely narrow inhomogeneous and homogeneous line widths (Fig.2).
Line broadening mechanisms can indeed be divided into two different types, inhomogeneous Γinh and homogeneous Γh broadening. The broadening of the inhomogeneous line width is due to static perturbations in the local environment of the optical center, such as microstructural strain, point defects and dislocations [38-39 These perturbations cause a small shift in the center frequencies of the optical centers, because the corresponding crystal field slightly changes. The inhomogeneous linewidth Γinh is then the combination of many homogeneously broadened lines centered at their different resonant frequencies. If inhomogeneous linewidths are narrow, it is possible, for example, to resolve small energy splittings. Typical values for inhomogeneous linewidths in rare earth doped crystals are 0.5-100 GHz [18]. In some special cases, where isotopically pure elements are used, inhomogeneous linewidths can be even narrower. For example, in 7LiYF4:170Er3+ inhomogeneous linewidths of 16 MHz were observed [18, 40] and it is believed that this is the narrowest optical ensemble linewidth ever observed in a solid. However, for frequency domain storage and processing it may be desirable to introduce disorder and increase the inhomogeneous linewidths, while maintaining a reasonable absorption coefficient and homogeneous linewidths as narrow as possible. This is because the figure of merit for such storage applications is Γinh/Γh. In contrast to inhomogeneous broadening, the homogeneous line broadening is caused by dynamical processes in the surrounding of the optical centers.

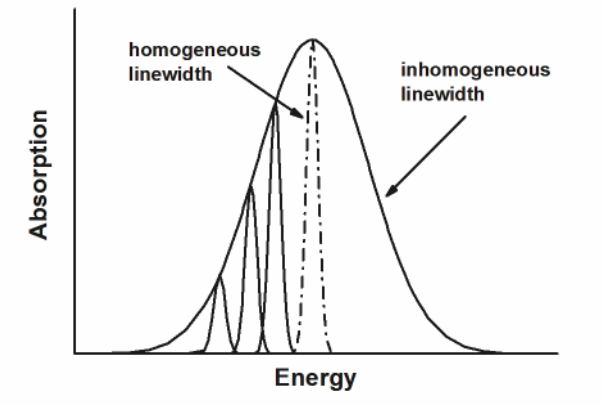

Figure 2. Example for inhomogeneous (Γinh) and homogeneous linewdiths (Γh).

These act, for example, as a perturbation on the activator ion's transition frequency. The homogeneous line width is related to the coherence lifetime by Γh = 1/πT2 and determined by several contributions which are explained in the following (equ. 2) [41-43]:

Γh = Γpop + Γion-ion + Γion-spin + Γphonon + ΓTLS (equ.2)

Γpop is the contribution of the excited state lifetime T1 (Γpop = 1/2πT1), which is usually not significant compared to the other contributions. Γion-ion is the contribution of excitation-induced instantaneous spectral diffusion (ISD) [44-46]. Optical excitation of the activator ions also leads to a change in its electric dipole moment and thus, a change in the local environment which can induce random frequency shifts. This contribution depends on the activator ion concentration and excitation intensity. A further contribution is the broadening caused by electron or nuclear spin flips, Γion-spin. To give an example, the contribution of yttrium nuclear spins in the homogeneous line broadening of Eu3+-doped Y2O3 is about 200-300 Hz [47]. For the fabrication of materials, it can therefore be useful to reduce electron and nuclear spins concentrations or to use external fields during manipulation in order to prevent spin flips. Γphonon is the phonon contribution. Depending on the ion level scheme, different temperature dependences of Γphonon can be observed due to Raman, Orbach or direct processes [15, 48].

The last remaining term is the contribution of dynamic fluctuations due to nearly equivalent configurations in the local environment, the so-called TLS contribution (two-level-system) ΓTLS. It is a measure of local disorder and can typically be observed in glasses [49]. While the inhomogeneous broadening can be measured at low temperature in a high-resolution absorption or photoluminescence experiment and, by scanning the absorption line with a narrow band laser, more sophisticated procedures are necessary to observe the homogeneous line broadening. Homogeneous linewidths or the corresponding coherence time cannot be directly measured in a simple absorption experiment.
There are two basic experiments, in the time or frequency domain, which are in principle equivalent. A convenient way to measure T2 and thus, the homogeneous linewidth, is to study photon echoes in the time domain. The experiment was initially developed by Hahn for nuclear spins [50] and then later transferred to the optical domain by Abella et al [51]. In the

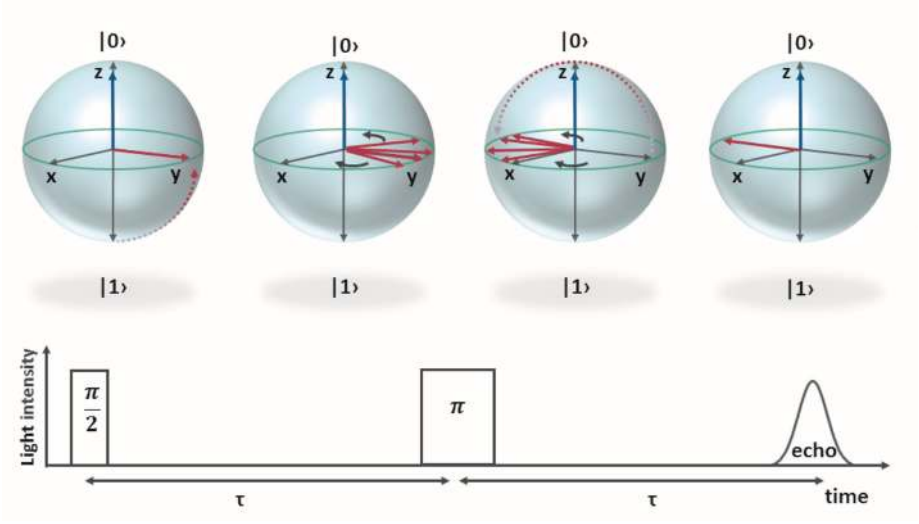

Figure 3. Schematic drawing of the two-pulse echo sequence. π/2, π and echo pulses are separated by a delay of τ.

simplest case, a two-pulse-sequence is used and the echo intensity Iecho decays [52] are recorded as a function of the delay between the π/2 and π pulses (see Fig. 3). A first pulse, the so-called π/2 pulse, creates a superposition, which can be described as a macroscopic dipole rotating in the xy-plane of a Bloch sphere. Now the excited ions show slightly different resonance frequencies, because they experience slightly different local environments. As a result, the ensemble dephases, which ultimately leads to a decrease of the intensity of the macroscopic emitting dipole. After a specified time interval , a second pulse, the so-called π-pulse, is shone onto the sample which results in a rotation of the Bloch vector (Fig. 2). Thus, the vectors on the plane will now rephase. After a delay 2τ from the initial pulse, the rephasing will be completed and a photon echo, an emission of light, can be observed. Only ions, which have not experienced any or only static perturbations during the whole echo sequence can participate in the echo emission and its intensity decay allows to determine T2 [15]. Alternatively, spectral hole burning (SHB) can be used in the frequency domain [15, 53]. For an inhomogeneously broadened transition, it is possible to bleach by optical pumping with a narrow-band laser source. In Fig. 4, this is shown for a very simple system with only two hyperfine ground state levels and one hyperfine excited state level and for simplicity it is assumed that the transition 1-3 under consideration is situated at the center of the inhomogeneous line.

At the start of the sequence, a smooth absorption profile is found when the line is scanned with a narrow laser at rather low laser power. Then, transition 1-3 is optically pumped and it is assumed that the ions from the upper level relax equally to 1 and 2. Now the ions populating level 2 are out of resonance and will therefore not be excited into level 3 anymore. Assuming a long lifetime of level 2, the whole population will be located in level 2 at the end. A low laser power scan can reveal a narrow hole in the absorption line. This hole is caused by the lack of ions in level 1, which could be excited into level 3 and its width is limited to twice the homogeneous linewidth of that transition. But since level 2 has a larger population than at the start of the sequence, a so-called anti-hole, an increased absorption for the transition from levels 2 to 3, is now observed. As illustrated in Fig. 4iii), the energy difference between 1 and 2 is often much smaller than the total width of the inhomogeneously broadened line. As a result, another class of ions will also be present, which show a transition 2'-3' at the same energy as the 1-3 transition for the first class of ions we were considering initially. Therefore, the 2'-3' transition is pumped as well, which results in another hole also positioned at the same place as the first (central hole) and a second anti-hole. A more detailed description of both techniques can also be found in Ref. [15]. For linewidth measurements, the disadvantage of SHB is the need for a very stable laser with a very narrow line. In contrast, for photon echoes the requirements concerning the laser are less restrictive. These techniques are not only useful to measure linewidths, but are also applied in quantum memories, even though the protocols applied are more complex. For example, hole burning techniques can be applied to prepare the system into a well-defined state used in further quantum memory experiments [54]. A memory protocol, which requires the creation of spectral features by spectral hole burning is, e.g., atomic frequency combs (AFCs) [55-57]. However, with the present short review we mainly aim at summarizing recent advances in the relevant material and we will therefore not illustrate the different memory protocols in detail. Beside the storage of photons, rare earth doped systems are also of great interest because they possess a nuclear spin and show long spin coherence times [58,59]. Since these systems exhibit both long

optical and spin coherence lifetimes, they are ideally suited for quantum interfaces. While the long optical coherence lifetimes allow communication via optical photons, data storage and processing can be carried out using nuclear spins. Furthermore, the electron spin also allows storing microwave photons and therefore interfacing with superconducting qubits [60] or microwave to optical conversion [61].

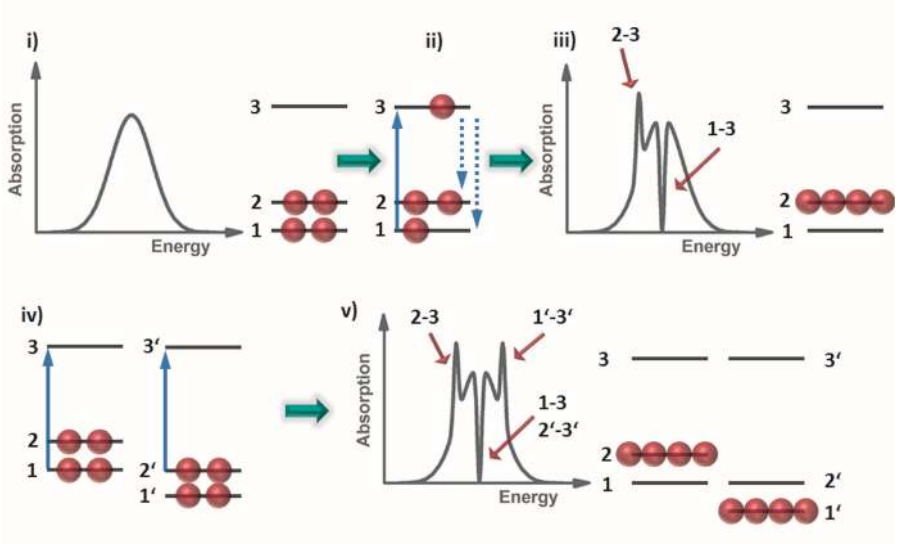

Figure 4. Schematic drawing of spectral hole burning (SHB).

3. Materials for quantum information processing

3.1. Rare Earth Doped Single Crystals

Coherence properties in rare earth doped crystals have already attracted attention for quantum information technologies. A number of promising materials is known and summaries can, for example, be found in Refs. [15, 18-22]. The inhomogeneous and homogeneous linewidths in rare earth single crystals can be extremely narrow at low temperatures. It is even believed that the 16 MHz inhomogeneous linewidth observed in 170Er3+:7LiYF4 is the narrowest optical ensemble linewidth ever observed in a solid, while a 25 MHz linewidth has been observed in isotopically purified EuCl3.H2O [62]. Very narrow homogeneous linewidths, in the 100 Hz range, have, for example, been observed in Y2SiO5:Er3+ (YSO:Er3+) and YSO:Eu3+ [63-65]. Other rare earth doped crystals with attractive coherence properties are, for example, YSO:Nd3+ [47], YSO:Pr3+ [66], Y3Al5O12:Tm3+ (YAG:Tm3+) [66, 67], LiNbO3:Tm3+ [68] or Y2O3:Eu3+ [69, 70]. YSO is a particularly attractive compound for low dephasing because of the low magnetic moment of the 100% abundant 89Y isotope and the low abundance of isotopes with non-zero spin for O and Si.

An abundant literature has appeared during the last few years on the growth, optical and magnetic spectroscopy and use of rare earth doped crystals for quantum information processing. In this review, we focus on three material-related topics that we find particularly

promising: Yb3+ doped crystals, nuclear spin coherence properties and structured bulk crystals.

Yb3+ has a 4f13 configuration that results in only two electronic multiplets, 2F7/2 and 2F5/2 separated by about 10000 cm-1. This has the advantage of reducing the number of optical transitions, compared to Eu3+ for example, and potentially increases the branching ratio of optical lines of interest. The excited state population lifetime is usually around 1 ms, which sets a limit on the homogeneous linewidth at about 150 Hz. The optical transition is located in the near infrared region, close to 1 µm, where tunable laser diodes with narrow linewidths are available. Yb3+ is also a paramagnetic ion and electron spin transitions can be used e.g. for storing microwave photons. Hyperfine transitions in isotopes 171 (I=1/2) and 173 (I=5/2) could provide additional storage possibilities. The 1/2 isotope is particularly interesting, since it corresponds to the simplest possible hyperfine structures. This could be very useful for tailoring the absorption for quantum memory protocols by optical pumping. Up to now, three systems have been investigated by high resolution spectroscopy: LiNbO3: Yb3+ [71], YAG:Yb3+ [72] and Y2SiO5:Yb3+ [73]. In the latter, a 50 ppm doped sample showed inhomogeneous linewidths of 1.7 and 2.2 GHz for the two sites and oscillator strengths of the order of 5-6 x 10-6, among the highest for rare earths in Y2SiO5 (Fig. 5). The branching ratio of the narrow lines between the lowest crystal field levels of the ground and excited multiplets were also large, between 5 and 10%, which is useful for coupling to optical cavities [74]. Magnetic properties were investigated by optical and electron resonance spectroscopies and the maximum g tensor eigenvalues were 6 and 3.3 for ground and excited states respectively. Yb3+ has therefore magnetic moments between those of Er3+ and Nd3+, as can be roughly expected from the J values of the multiplets. Ground state hyperfine structures have also been measured and exhibit total splittings on the order of a few GHz at zero magnetic field, suitable for absorbing microwave photons. In addition, simulations suggest that transitions partially insensitive to magnetic field fluctuations could be obtained by applying small magnetic fields.

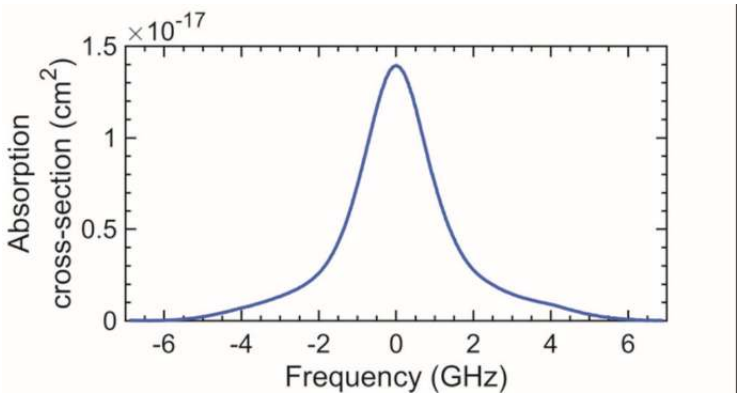

Figure 5 Absorption spectrum of Y2SiO5:Yb3+ around 981.463 nm (vacuum) for light polarized along b.

Such transitions should have long coherence lifetimes, since magnetic perturbations, from other Yb3+ ions or Y host spins, are expected to be the main source of dephasing in this system. In YAG: Yb3+, a detailed study of the optical transition at 968 nm was performed under various temperatures and magnetic fields [72]. Doped at 500 ppm, the crystal showed a

surprisingly narrow inhomogeneous line, 3.6 GHz, compared to other rare earth doped in YAG. 0.5% YAG:Tm3+ for example has a linewidth close to 20 GHz, which is generally explained by the high concentration of antisites defects in this host [75]. It is also a low value compared to the ones observed for Y2SiO5 in a sample 10 times less doped (see above). Photon echoes were used to measure homogeneous linewidths, which were found to be as low as 5 kHz under a field of 2.5 T. This value was limited by interactions between Yb3+ spins, as confirmed by non-exponential echo decays. In lower doped samples, much narrower linewidths could be obtained. The third investigated system is LiNbO3:Yb3+ [71]. Here also, despite the high Yb3+ concentration of 1000 ppm, and the charge compensation needed for Yb3+ doping, linewidths as low as 30 GHz are observed, whereas 180 GHz have been reported in LiNbO3:Er3+ at 50 ppm doping level [22]. A detailed study of spectral hole burning has been carried out, but at 9 K, so that the properties at the temperatures usually used for quantum processing experiments are not known yet. Although these results show that Yb3+ doped crystals are promising materials, further studies, especially on the dynamical properties of optical and spin transitions will be required to completely assess their usefulness for quantum technologies.
Nuclear spins are a very important resource for rare earth ions because they can provide transitions with very long coherence lifetimes, to which optical or microwave excitations can be transferred. In this respect, optical quantum memories using nuclear spins have been reported in Eu3+ [76], [77] and Pr3+ 78, 79] doped Y2SiO5 crystals. Several studies also focused on the control of spin coherences by magnetic or electric fields. A first example is given by investigations of 151Eu3+ isotope in Y2SiO5. The zero magnetic field hyperfine structure of the ground state level (7F0) consists in three doubly degenerate levels separated by a few tens of MHz, because of the quadrupole interaction between the I=5/2 nuclear spin and electric field gradients [43].

Experiments were carried out using optically detected magnetic resonance [81]. More precisely, the crystal is placed in a coil which can produce efficient RF excitations of nuclear spins. When spin coherence needs to be detected, a lase probe is shone on the sample, creating an optical coherence that combines with the spin one. This induces a second optical field that interferes with the probe beam and produces a beating at the RF frequency on a photodiode output signal with an amplitude proportional to the spin coherence. This excitation and detection scheme is used in spin echo sequences for T2 measurements. At zero magnetic field, spin T2 for the 34 MHz transition in Y2SiO5:151Eu3+ is 19 ms 82, 83], and 26 ms under 4.8 mT. These values can be observed up to 16 K [84], and are limited by interactions with 89Y nuclear spins [106]. A first technique to decrease these interactions, called dynamical decoupling, is to use trains of RF π pulses [85]. For short enough delays between these pulses, the fluctuations due to Y spin flips are slow enough to be refocused, in the same way as inhomogeneous broadening is refocused by the π pulse in a 2-pulse echo. This technique effectively extends coherence lifetimes and T2 up to nearly 500 ms were demonstrated, an 18-fold increase compared to the 2-pulse echo T2 [83]. This technique was also shown to work for single photon level excitations, a key result for application to quantum memories [77]. At the expense of a more complex setup and energy level schemes, much longer values can be obtained. By applying specific magnetic fields, transitions that are insensitive to magnetic perturbations, the so-called ZEFOZ (zero first order Zeeman shift) transition [86], can be created because of the addition of quadrupole and Zeeman interactions. Combined with dynamical decoupling, this technique resulted in coherence lifetimes of 6 hours, a record value

for optically addressable nuclear spins [87]. Spin T2 extensions obtained in a similar way have been reported in other systems like YAG:Tm3+ [78] and Y2SiO5:Pr3+ [89, 90]. The influence of electric fields has also been measured in Y2SiO5:151Eu3+ [91]. It is due to a change in the electric field gradients surrounding the nucleus which causes a shift in the hyperfine level energies. These shifts turn to be very small, about 1 Hz/(V/cm), whereas optical transitions shifts are nearly five orders of magnitude larger. Nevertheless, they can be useful to manipulate spin state because their effect can accumulate over long coherence lifetimes. This has been used to design a low noise and broadband quantum memory protocol that can be used for optical, electron and nuclear spin transitions [92].
Paramagnetic ions have also been recently investigated. It has been shown that high magnetic fields (7 T) can result in coherence lifetime of the order of 1 s for hyperfine transitions in Y2SiO5:167Er3+ [93], which is of great interest for quantum memories at the 1.5 µm telecom wavelength. In this case, the strong fields freeze the spin on the lower electron spin multiplet which dramatically reduces Er3+-Er3+ magnetic interactions. Nuclear spins can also be used in connection with electron spins to provide storage for microwave excitations. This was demonstrated in Y2SiO5:145Nd3+, where electron nuclear double resonance, ENDOR, was used to investigate nuclear spin coherence lifetimes. Values up to 10 ms at 5 K, under a field of 500 mT, were measured, at the level of the longest T2 obtained for non-paramagnetic rare earth ions [59]. They could be significantly increased by using dynamical decoupling and/or ZEFOZ techniques. Moreover, high fidelity coherence transfer between electron and nuclear spins, was demonstrated by quantum state tomography. This suggest that this crystal could be used for microwave quantum storage, with an additional optical interfacing.

Crystals can be structured to create waveguides or optical cavities, which is of interest for applications in quantum information processing. Indeed, light-matter interactions can be strongly enhanced in high-quality optical cavities, i.e. in which photons have a long lifetime. This results in various effects like the enhancement of the fluorescence intensity for transitions in resonance with cavity, the so-called Purcell effect [94]. Cavities are useful for e.g. single ion detection, as well as fast coherent driving of transitions over a large bandwidth. This could lead to new types of quantum memories with e.g. processing capabilities. High-quality cavities can be realized directly in rare earth doped crystals using focused ion beam (FIB) milling (Fig. 6) [95]. Here FIB allows one to create very precise nano-structures in a YVO4:Nd3+ crystal that act as an optical resonator with a quality factor (ratio between resonance frequency and cavity linewidth) up to 10000. A key point is that the coherence lifetime of Nd3+ ions is unchanged by the cavity fabrication, despite the possibility of crystal damage from the ion beam resulting in additional dephasing through defects or disorder.

3.2. Waveguides

Waveguides are also an important element of integrated optics. They can be obtained in several different ways, that often depend on the material. A recent result obtained in LiNbO3 waveguides obtained by ion exchange is the strong increase in coherence lifetime at temperatures below 1 K [97]. Whereas at 3.5 K, T2 is about 1.5 µs, it reaches 117 µs at 0.8 K and is equivalent to values observed in the bulk. The reasons for this behavior are not completely understood yet, but could be linked to the Ti4+ ions that are indiffused in the crystal to modify the refractive index. Another type of waveguides, obtained by femtosecond laser writing, have been investigated in Y2SiO5:Pr3+ [98]. In this case, coherence lifetimes,

measured by two pulse photon echoes, were found to be similar to the bulk values at 3.5 K. Inhomogeneous linewidths were close to the bulk, too, showing that the effect of the writing pulses, which are on the sides of the guiding area, did not affect Pr3+ ions. Optical memories have been demonstrated in both types of these waveguides [97, 98]. An alternative to structure the crystals themselves consists in coupling rare earth ions to waveguide or cavities deposited on the crystal surface through evanescent waves. This has been reported in Pr3+ [99] and Er3+ [100] doped Y2SiO5 and Yb3+ doped glasses [101].

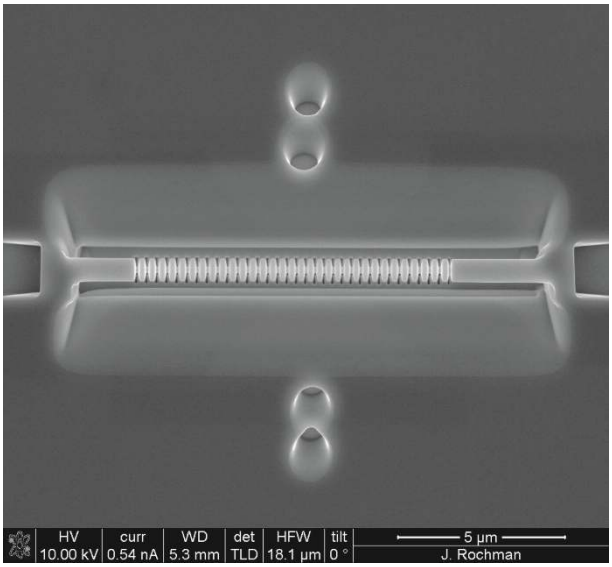

Figure 6. Scanning electron microscope image of a one-sided nanobeam optical cavity described in Ref. [95, 96]. Photography courtesy of Jake Rochman, and Andrei Faraon, California Institute of Technology.

3.3. Rare Earth Doped Powders and Ceramics

Even until the last decade, transparent high quality optical samples, such as single crystals, fibres or glasses were believed to be necessary for the measurements of photon echoes. Therefore, highly scattering polycrystalline powders were only studied using spectral hole burning (SHB), like for example Y2O3:Eu3+ or Eu2O3 nanoparticles [102-104]. These measurements often suffer from the severe disadvantage that the minimum hole width at low temperatures can be laser-limited and the real hole widths not resolved. Thus, measurements of narrow homogeneously broadened lines require a laser with a very narrow line. In 2011, Beaudoux et al [105] were able to observe for the first time photon echoes on the 3H4-1D2 transition of Pr3+ in a highly-scattering powder obtained by grinding a Y2SiO5:Pr3+ crystal. Photon echoes could be recorded while heterodyning with a reference field, a technique that enormously increases the signal-to-noise ratio. This discovery finally opened up the possibility to measure optical coherence lifetimes in polycrystalline scattering samples. Later on, Perrot et al [106] measured the temperature dependence of the homogeneous linewidth with a two-pulse-photon-echo experiment on the 7F0-5D0 transition in Y2O3:Eu3+ nanocrystals for the first time. This is of interest for e.g. single rare earth detection [107, 108] and manipulation, opening the way to e.g. quantum memories with processing capabilities. The particles were obtained by a solvothermal methods followed by calcination. At 1.3 K, a homogeneous

linewidth of 86 kHz could be resolved for 60 nm Eu3+-doped Y2O3 particles. Even if the materials cannot be directly compared, because in the earlier works the monoclinic phase was present, whereas Perrot et al studied the body-centred cubic phase, it is still worth to mention that the homogeneous linewidths found by photon-echo measurements are by a factor of 100 narrower than those found by spectral hole burning in the earlier experiment [102]. A measurement via spectral hole burning, would only yield limited information, because the laser showed a frequency jitter of several MHz, which is much broader than the observed homogeneous linewidth. These results showed that Eu3+-doped nanoparticles may be of interest for quantum optics on the submicron scale. Further studies then revealed that Y2O3:Eu3+ particles of around 150 nm size can show inhomogeneous linewidths comparable to single crystals [109, 110]. In order to identify the mechanisms responsible for the optical homogeneous broadening and to clarify if the minimum line width is fundamentally limited compared to single crystals, further temperature-dependent and magnetic-field-dependent photon-echo and spectral hole burning studies on Y2O3:Eu3+ particles were carried out by Bartholomew et al [111]. In 0.5% Eu3+-doped Y2O3 with a particle size of about 400 nm and crystallite sizes of about 130 nm obtained by homogeneous precipitation followed by calcination, homogeneous linewidths of about 45 kHz at low temperatures were found. In contrast to previous studies on nanoparticles, the authors were able to demonstrate that the broadening due to size-dependent phonon interaction is not significantly contributing to the homogenous line width. Analogous to bulk single crystals, the dominating contributions to the homogenous broadening at higher temperatures are two phonon Raman processes. In the temperature range between 5 and 10 K they observed mainly broadening due to TLS (two level system). This phenomenon is caused by dynamic fluctuations due to nearly equivalent configurations, as usually observed in disordered materials such as glasses [112]. Up to a usually smaller degree than in glasses, optical dephasing due to disorder modes can also take place in crystals [113, 114]. The remaining broadening at very low temperatures was mainly attributed to surface charge fluctuations that cause a rapidly varying electric field. Thus, the authors concluded that the transition is broadened by linear Stark interactions. In conclusion, this recent result raises hopes that quantum optical devices can be fabricated even on the submicron scale. Furthermore, Lutz et al [115] suggest nano-structuring of rare earth doped materials as a tool to influence the phonon density of states. Even at low temperatures, the so-called spin-lattice relaxation (thermalization of spins through the interaction with lattice phonons) limits the lifetimes of spin states. Additionally, lattice vibrations also limit coherence times by contributing to spectral diffusion [116] and two-phonon elastic scattering processes [117]. Lutz et al propose to overcome these problems by tailoring the phonon density of states, which is achieved by using nano-structured materials. Suppression of direct phonon processes can either be reached using nanocrystalline powders with a cut-off frequency in their phonon density of states or tailored phononic band gap crystals. The later requires the growth of high-quality thin films. Here, the authors focus on the Er3+-doped materials Y2SiO5, LiNbO3 and KTiOPO4. The Er3+-transition 4I15/2 – 4I13/2 at approx. 1530 nm, which is also relevant for telecommunication, is investigated and the authors present numerical calculations of phonon densities and optical linewidths for Er3+-doped Y2SiO5. The results suggest that this approach could increase the performance of optical quantum memories operating at telecommunication wavelengths. Beside the above-mentioned experimental studies using the bottom-up approach for the particle syntheses and the theoretical modelling, first investigations using the top-down approach have also been carried out by Lutz et al. In Er3+-doped LiNbO3 powders, the coherence properties were studied after mechanical

processing and annealing [118]. Not very surprisingly, it was found that mechanical grinding rapidly degrades the coherence properties compared to bulk single crystals samples. Coherence behaviour comparable to amorphous materials can be observed and the homogeneous linewidth can broaden by three orders of magnitude. In contrast, annealing at high temperatures can improve the coherence properties and reduce the line widths again to values less than 10 kHz, which is close to the bulk single crystal line width. In a further study on Tm3+-doped Y3Al5O12 [119] it was also found that mechanical treatment degrades the coherence properties of a material, whereas thermal annealing can improve them. These results underline the importance of controlling the mechanical and thermal treatments of the sample and avoiding the formation of lattice strain and defects. Additionally, to the recent investigations on powders of Y2O3, the 7F0-5D0 Eu3+ transition has recently also been studied in transparent ceramics [41, 120-122]. Since transparent ceramics are promising materials to replace bulk single crystals in lasers [123], they could also replace crystals in some quantum technologies. Here, the ceramics were obtained by HIP (hot isostatic pressing) treatment of pellets obtained from Eu2O3 and Y2O3 nanocrystalline powders. In 2013, when coherence properties in transparent ceramics were studied for the first time, a homogeneous linewidth of about 60 kHz was found [120] and the dephasing was attributed to magnetic impurities and defects from the synthesis process. A better control of the preparation then yielded homogeneous linewidths below 10 kHz [41], comparable to single crystals. Additionally, lifetimes of spectral holes of more than 15 min could be observed. Kunkel et al [121, 122] then studied the influence of annealing treatments of transparent ceramics after the hot isostatic pressing process. Different types of defects depending on the annealing atmosphere and temperatures could be identified, which influence the homogeneous linewidth and its temperature-dependence. Homogeneous linewidths between 3 and 10 kHz were found for the different samples. As an example, the temperature-dependence of a Eu3+-doped Y2O3 transparent ceramic, which had been annealed under air at high temperature after the hot isostatic pressing process is shown in Fig. 7.

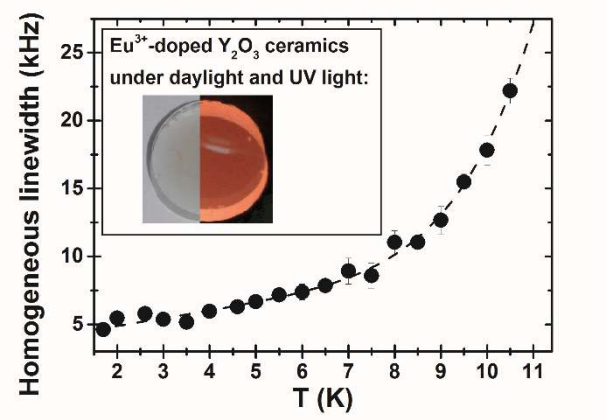

Figure 7. Temperature dependence of the homogeneous linewidths (Γh) of the 7F0-5D0 Eu3+ transition in a Y2O3 transparent ceramic.

It was concluded that both local disorder as well as magnetic impurities play a role. A better control on the material's processing will enable the fabrication of ceramics with even better coherence properties and open up new possibilities for the design of quantum devices. A

comparison of the homogeneous linewidths at low temperatures for the 7F0-5D0 Eu3+ -transition in Y2O3 in its different forms is shown in Fig. 8.

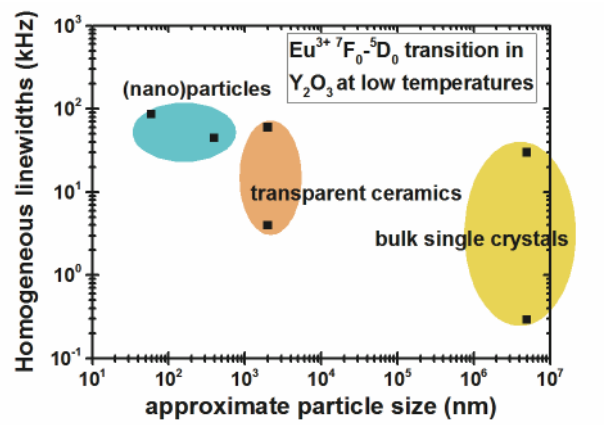

Figure 8. Homogeneous linewidths (Γh) of the 7F0-5D0 Eu3+ transition with respect to approximate particle sizes in Y2O3.

Besides the optical coherence properties, also the inhomogeneous linewidths and coherence time of nuclear spin transitions were studied in Eu3+-doped transparent Y2O3 ceramics [58] by an all-optical spin echo technique. Karlsson et al found that the coherence times are constant up to 18 K, which relaxes the requirements on the cooling system. Nuclear spin echoes were recorded for the 1/2-3/2 and 3/2-5/2 ground state transition of 151Eu3+ as well as for the 1/2-3/2 transitions of 153Eu3+ and the values found here are comparable to the best rare earth doped bulk single crystal. Recently, coherence properties were also studied in Er3+-doped Y2O3 transparent ceramics [124] and a homogeneous linewidth of 11.2 kHz at low temperatures was found for the 4I13/2 – 4I15/2 transition in a 0.65 T magnetic field. The combination of coherence properties and the good optical transparency in the wavelength range of 1000-2000 nm make them a promising system for quantum memories using telecommunication wavelengths. A further system, which was recently studied, are opaque Tm3+-and Sc3+-doped Y3Al5O12 ceramics prepared by solid state reactions with 0.5% Tm3+ and Sc3+-concentrations from 0-6% [75]. Ferrier et al used Sc3+-doping in order to increase the Tm3+ inhomogeneous linewidth in Y3Al5O12 ceramics to obtain a larger bandwidth for signal processing applications and show that the homogeneous linewidths are comparable to those in single crystals.

4. Conclusion and Outlooks

Quantum information processing currently represents a very important and active research field, offering unprecedented computational capacities and close to unconditional communication security using quantum cryptography. A prerequisite for quantum information processing is the availability of materials with good coherence properties. Among the material classes studied so far, rare earth doped dielectric host lattices are one of the most promising. The narrow f-f-transitions of trivalent rare earth ions can cover the visible and the IR range including the telecom wavelength at 1.5 µm, and, more importantly, at low temperatures, these systems often show long optical and spin coherence states. Using mainly single crystals, it could be shown during recent years that spin states can have long coherence

lifetimes and be manipulated using magnetic and electric fields. New systems have been investigated, like ytterbium doped crystals, with promising optical and spin properties, whereas structuring opens promising perspectives for stronger light matter interactions and integrated optics. Beside single crystals, progress has been made in rare earth doped transparent ceramics, and rare earth doped polycrystalline (nano) powders. Further progress in fabrication, e.g. nano-structuring, nanoparticles, or thin films will offer new possibilities for the design of quantum light-matter interfaces, long time storage memories and scalable processors. They may also benefit to other applications that rely on narrow transitions like laser stabilization, signal processing or medical imaging.

Acknowledgements

The authors would like to thank the Bavarian-French Academy Center for a mobility aid for their French-German collaboration. Furthermore, Ph. G. would like to thank for funding by European Union's Horizon 2020 research and innovation program under grant agreement no. 712721 (NanOQTech), ANR under grant agreements no. 145-CE26-0037-01 (DISCRYS), and Nano'K project RECTUS. N. K. would like to thank the Fonds der Chemischen Industrie for a Liebig Fellowship, the Deutsche Foschungsgemeinschaft (DFG KU 3427/1-1) and Prof. Fässler for hosting our junior research group. Furthermore, we thank Sacha Welinski for photographs of the single crystals used in our TOC graphic and John G. Bartholomew for fruitful discussions.

Keywords: rare earths ions • quantum memory • quantum information processing • photon echo • waveguide • nanoparticle

[1] S. Schmiechen, P. Pust, P. J. Schmidt, W. Schnick, Nachr. Chem. 2014, 62, 847-851.
[2] G. Blasse, B. C. Grabmaier in Luminescent Materials, Springer, Berlin, 1994.
[3] T. Jüstel, H. Nikol, C. Ronda, Angew. Chem. Int. Ed. 1998, 37, 3084-3103.
[4] H. A. Höppe, Angew. Chem. Int. Ed. 2009, 48, 3572-3582.
[5] W. Schnick, Phys. Status Solidi RRL 2009, 3, A113-A114.
[6] P. Pust, P. J. Schmidt, W. Schnick, Nature Mat. 2015, 14, 454-458.
[7] R. Mueller-Mach, G. Mueller, M. R. Krames, H. A. Höppe, F. Stadler, W. Schnick, T. Juestel, P. Schmidt, Phys. Stat. Sol. (a) 2005, 202, 1727-1732.
[8] T. Schlieper, W. Milius, W. Schnick, Z. Anorg. Allg. Chem. 1995, 621, 1380-1384.
[9] H. Huppertz, W. Schnick, Acta Cryst. C 1997, 53, 1751-1753.
[10] W. Schnick, H. Huppertz, R. Lauterbach, J. Mater. Chem. 1999, 9, 289-296.
[11] H. A. Höppe, H. Lutz, P. Morys, W. Schnick, A. Seilmeier, J. Phys. Chem. Sol. 2000, 61, 2001-2006.
[12] M. Zeuner, S. Pagano, W. Schnick, Angew. Chem. Int. Ed. 2011, 50, 7754-7775.
[13] P. Pust, V. Weiler, C. Hecht, A. Tücks, A. S. Wochnik, A.-K. Henß, D. Wiechert, C. Scheu, P. J. Schmidt, W. Schnick, Nature Mat. 2014, 13, 891-896.
[14] C. Poesl, W. Schnick, Chem. Mater. 2017, 29, 3778-3784.
[15] Ph. Goldner, A. Ferrier, O. Guillot-Noël in Handbook on the Physics and Chemistry of Rare Earth, Vol 46 (Eds.: J.-C. G. Bünzli, V. K. Pecharsky). North Holland, Amsterdam, 2015, 1-78.
[16] W. Tittel, T. Chanelière, R. L. Cone, S. Kröll, S. A. Moiseev, M. Sellars, Laser & Photon. Rev. 2010, 4, 244-267.
[17] A. I. Lvovsky, B. C. Sanders, W. Tittel, Nature Phot. 2009, 3, 706-714.

[18] R. M. Macfarlane, J. Lumin. 2002, 100, 1-20.
[19] Y. Sun, C. W. Thiel, R. L. Cone, R. W. Equall, R. L. Hutcheson, J. Lumin. 2002, 98, 281-287.
[20] Y. Sun in Spectroscopic Properties of Rare Earth in Optical Materials (Eds.: G. Liu, B. Jacquier), Springer Berlin and Tsinghua University Press 2005, pp. 379-429.
[21] R. M. Macfarlane, J. Lumin. 2007, 125, 156-174.
[22] C. W. Thiel, T. Böttger, R. L. Cone, J. Lumin. 2011, 131, 353-361.
[23] M. P. Hedges, J. J. Longdell, Y. Li, M. J. Sellars, Nature 2010, 465, 1052-1056.
[24] I. Usmani, M. Afzelius, H. de Riedmatten, N. Gisin, Nature Comm. 2010, 1, 1-7.
[25] C. Clausen, I. Usmani, F. Bussières, N. Sangouard, M. Afzelius, H. de Riedmatten, N. Gisin, Nature 2011, 469, 508-511.
[26] I. Usmani, C. Clausen, F. Bussières, N. Sangouard, M. Afzelius, N. Gisin, Nature Phot. 2012, 6, 234-237.
[27] J. Stolze, D. Suter in Quantum Computing: A short course from theory to experiment, 2nd edition Wiley-VCH Berlin 2008.
[28] T. D. Ladd, F. Jelezko, R. Laflamme, Y. Nakamura, C. Monroe, J. L. O'Brien, Nature 2010, 464, 45-53.
[29] R. Blatt, C. F. Roos, Nature Phys. 2012, 8, 277-284.
[30] J. Clarke, F. K. Wilhelm, Nature 2008, 453, 1031-1042.
[31] T. Chanelière, D. N. Matsukevich, S. D. Jenkins, S. Y. Lan, T. A. B. Kennedy, A. Kuzmich, Nature 2005, 438, 833-836.
[32] J. J. L. Morton, A. M. Tyryshkin, R. M. Brown, S. Shankar, B. W. Lovett, A. Ardavan, T. Schenkel, E. E. Haller, J. W. Ager, S. A. Lyon, Nature 2008, 455, 1085-1088.
[33] J. Wrachtrup, F. Jelezko, J. Phys.: Condens. Matter 2006, 18, S807-S824.
[34] J. N. Becker, J. Görlitz, C. Arend, M. Markham, C. Becher, Nature Comm. 2016, 7, 1-6.
[35] B. Pingault, D.-D. Jarausch, C. Hepp, L. Klintberg, J. N. Becker, M. Markham, C. Becher, M. Atatüre, Nature Comm. 2017, 8, 1-7.
[36] T. E. Northup, R. Blatt, Nature Phot. 2014, 8, 356-363.
[37] N. Ohlsson, R. Krishna Mohan, S. Kröll, Opt. Commun. 2002, 201, 71-77.
[38] A. M. Stoneham, Proc. Phys. Soc. London 1966, 89, 909-921.
[39] A. M. Stoneham, Rev. Mod. Phys. 1969, 41, 82-108.
[40] E. P. Chukalina, M. N. Popova, S. L. Korableva, R. Yu. Abdusabirov, Phys. Lett. A 2000, 269, 348-350.
[41] N. Kunkel, J. Bartholomew, L. Binet, A. Ikesue, Ph. Goldner, J. Phys. Chem. C 2016, 120, 13725-13731.
[42] R. M. Macfarlane, R. M. Shelby in Spectroscopy of Solids Containing Rare Earth Ions (Eds. A. A. Kaplyanskii, R. M. Macfarlane) North Holland, Amsterdam, 1987, p. 51.
[43] R. W. Equall, R. L. Cone, R. M. Macfarlane, Phys. Rev. B: Condens. Matter Mater. Phys. 1995, 52, 3963-3969.
[44] J. Huang, J. M. Zhang, A. Lezama, T. W. Mosberg, Phys. Rev. Lett. 1989, 63, 78-81.
[45] G. K. Liu, R. L. Cone, M. F. Joubert, B. Jacquier, J. L. Skinner, J. Lumin. 1990, 45, 387-391.
[46] G. K. Liu, R. L. Cone, Phys. Rev. B 1990, 41, 6193-6200.
[47] R. M. Macfarlane, R. M. Shelby, Opt. Commun. 1981, 39, 169-171.
[48] D. E. McCumber, M. D. Sturge, J. Appl. Phys. 1963, 34, 1682-1684.
[49] M. M. Broer, B. Golding, J. Lumin. 1984, 31-33, 733-737.
[50] E. Hahn, Phys. Rev. 1950, 80, 580-594.

[51] I. D. Abella, N. A. Kurnit, S. R. Hartmann, Phys. Rev. 1966, 141, 391-406.
[52] R. G. Brewer, R. L. Shoemaker, Phys. Rev. A: At., Mol., Opt. Phys. 1972, 6, 2001-2007.
[53] L. E. Erickson, Phys. Rev. B 1977, 16, 4731-4736.
[54] B. Lauritzen, N. Timoney, N. Gisin, M. Afzelius, H. de Riedmatten, Y. Sun, R. M. Macfarlane, R. L. Cone, Phys. Rev. B 2012, 85, 115111 (10pp).
[55] M. Bonarota, J.-J. Le Gouët, T. Chanelière, N. J. Phys. 2011, 13, 01013 (13pp).
[56] M. Afzelius, C. Simon, H. de Riedmatten, N. Gisin, Phys. Rev. A 2009, 79, 052329 (9pp).
[57] C. Clausen, I. Usmani, F. Bussières, N. Sangouard, M. Afzelius, H. de Riedmatten, N. Gisin, Nature 2011, 469, 508-511.
[58] J. Karlsson, N. Kunkel, A. Ikesue, A. Ferrier, Ph. Goldner, J. Phys.: Condens. Matter 2017, 29, 125501 (7pp).
[59] G. Wolfowicz, H. Maier-Flaig, R. Marino, A. Ferrier, H. Vezin, J. J. L. Morton, Ph. Goldner, Phys. Rev. Lett. 2015, 114, 170503 (5pp).
[60] S. Probst, H. Rotzinger, S. Wünsch, P. Jung, M. Jerger, M. Siegel, A. V. Ustinov, P. A. Bushev, Phys. Rev. Lett. 2013, 110, 157001 (5pp), 2013.
[61] L. A. Williamson, Y.-H. Chen, J. J. Longdell, Phys. Rev. Lett. 2014, 113, 203601 (5pp).
[62] R. L. Ahlefeldt, M. R. Hush, M. J. Sellars, Phys. Rev. Lett. 2016, 117, 250504 (6pp).
[63] R. W. Equall, Y. Sun, R. L. Cone, Phys. Rev. Lett. 1994, 72, 2179-2182.
[64] F. Könz, Y. Sun, C. W. Thiel, R. L. Cone, R. W. Equall, R. L. Hutcheson, R. M. Macfarlane, Phys. Rev. B: Condens. Matter Mat. Phys. 2003, 68, 085109 (9pp).
[65] T. Böttger, C. W. Thiel, R. L. Cone, Y. Sun, Phys. Rev. B.: Condens. Matter Mat. Phys. 2009, 79, 115104 (8pp).
[66] R. M. Macfarlane, Opt. Lett. 1993, 22, 1958-1960.
[67] O. Guillot-Noël, P. Goldner, E. Antic-Fidancev, J.-L. Le Gouët, Phys. Rev. B: Condens. Matter Mat. Phys. 2005, 71, 174409 (15pp).
[68] C. W. Thiel, Y. Sun, T. Böttger, W. R. Babbit, R. L. Cone, J. Lumin. 2010, 130, 1598-1602.
[69] R. M. Macfarlane R. M. Shelby, Opt. Comm. 1981, 39, 169-171
[70] W. R. Babbit, A. Lezama, T. W. Mossberg, Phys. Rev. B: Condens. Matter Mat. Phys. 1989, 39, 1987-1992.
[71] Z. Kis, G. Mandula, K. Lengyel, I. Hajdara, L. Kovacs, M. Imlau, Opt. Mat. 2014, 37, C, 845–853.
[72] T. Böttger, C. W. Thiel, R. L. Cone, Y. Sun, A. Faraon, Phys. Rev. B: Condens. Matter Mat. Phys. 2016, 94, 045134–13.
[73] S. Welinski, A. Ferrier, M. Afzelius, P. Goldner, Phys. Rev. B: Condens. Matter Mat. Phys. 2016, 94, 155116 (8pp).
[74] D. L. McAuslan, J. J. Longdell, M. J. Sellars, Phys. Rev. A: At., Mol., Opt. Phys. 2009, 80, 062307 (9pp).
[75] A. Ferrier, S. Ilas, Ph. Goldner, A. Louchet-Chauvet, J. Lumin. 2018, 194, 116-122.
[76] C. Laplane, P. Jobez, J. Etesse, N. Gisin, M. Afzelius, Phys. Rev. Lett. 2017, 118, 210501 (5pp).
[77] P. Jobez, C. Laplane, N. Timoney, N. Gisin, A. Ferrier, P. Goldner, M. Afzelius, Phys. Rev. Lett. 2015, 114, 230502 (5pp).
[78] A. Seri, A. Lenhard, D. Rieländer, M. Gündoğan, P. M. Ledingham, M. Mazzera, H. de Riedmatten, Phys. Rev. X 2017, 7, 021028 (7pp).

[79] B. Albrecht, P. Farrera, G. Heinze, M. Cristiani, H. de Riedmatten, Phys. Rev. Lett.2015, 115, 160501 (6pp).
[80] K. Kutluer, M. F. Pascual-Winter, J. Dajczgewand, P. M. Ledingham, M. Mazzera, T. Chanelière, H. de Riedmatten, Phys. Rev. A: At., Mol., Opt. Phys. 2016, 93, 040302 (5pp).
[81] J. Mlynek, N. C. Wong, R. G. DeVoe, E. S. Kintzer, and R. G. Brewer, Phys. Rev. Lett. 1983, 50, 993–996.
[82] A. L. Alexander, J. J. Longdell, M. J. Sellars, J. Opt. Soc. Am. B 2007, 24, 2479–2482.
[83] A. Arcangeli, M. Lovrić, B. Tumino, A. Ferrier, P. Goldner, Phys. Rev. B: Condens. Matter Mat. Phys. 2014, 89, 184305 (6pp).
[84] A. Arcangeli, R. Macfarlane, A. Ferrier, and P. Goldner, Phys. Rev. B: Condens. Matter Mat. Phys. 2015, 92, 224401 (6pp).
[85] L. Viola, S. Lloyd, Phys. Rev. A: At., Mol., Opt. Phys. 1998, 58, 2733–2744.
[86] E. Fraval, M. J. Sellars, J. J. Longdell, Phys. Rev. Lett. 2004, 92, 077601 (4pp).
[87] M. Zhong, M. P. Hedges, R. L. Ahlefeldt, J. G. Bartholomew, S. E. Beavan, S. M. Wittig, J. J. Longdell, and M. J. Sellars, Nature 2015, 517, 177–180.
[88] M. Pascual-Winter, R. C. Tongning, T. Chanelière, J.-L. Le Gouët, Phys. Rev. B: Condens. Matter Mat. Phys. 2012, 86, 184301 (9pp).
[89] J. J. Longdell, E. Fraval, M. J. Sellars, and N. B. Manson, Phys. Rev. Lett. 2005, 95, 063601 (4pp).
[90] G. Heinze, C. Hubrich, and T. Halfmann, Phys. Rev. Lett. 2013, 111, 033601 (4pp).
[91] R. M. Macfarlane, A. Arcangeli, A. Ferrier, P. Goldner, Phys. Rev. Lett. 2014, 113, 157603 (5pp).
[92] A. Arcangeli, A. Ferrier, P. Goldner, Phys. Rev. A: At., Mol., Opt. Phys. 2016, 93, 062303 (6pp).
[93] M. Rančič, M. P. Hedges, R. L. Ahlefeldt, M. J. Sellars, Nat. Phys. 2017, 5, 4254 (1-6pp).
[94] H. Kaupp, C. Deutsch, H.-C. Chang, J. Reichel, T. W. Hänsch, and D. Hunger, Phys. Rev. A: At., Mol., Opt. Phys. 2013, 88, 053812 (8pp).
[95] T. Zhong, J. M. Kindem, E. Miyazono, and A. Faraon, Nat. Commun. 2015, 6, 8206 (6pp).
[96] T. Zhong, J. M. Kindem, J. G. Bartholomew, J. Rochman, I. Craiciu, E. Miyazono, M. Bettinelli, E. Cavalli, V. Verma, S. W. Nam, F. Marsili, M. D. Shaw, A. D. Beyer, A. Faraon, Science 2017, 357, 1392-1395.
[97] N. Sinclair, D. Oblak, C. W. Thiel, R. L. Cone, and W. Tittel, Phys. Rev. Lett. 2017, 118, 100504–5.
[98] G. Corrielli, A. Seri, M. Mazzera, R. Osellame, H. de Riedmatten, Phys. Rev. Applied 2016, 5, 054013 (7pp).
[99] S. Marzban, J. G. Bartholomew, S. Madden, K. Vu, M. J. Sellars, Phys. Rev. Lett. 2015, 115, 013601 (5pp).
[100] E. Miyazono, I. Craiciu, A. Arbabi, T. Zhong, A. Faraon, Opt. Express 2017, 25, 2863–2871.
[101] D. Ding, L. M. C. Pereira, J. F. Bauters, M. J. R. Heck, G. Welker, A. Vantomme, J. E. Bowers, M. J. A. de Dood, D. Bouwmeester, Nat. Photonics 2016, 1–5.
[102] K. S. Hong, R. S. Meltzer, B. Bihari, D. K. Williams, B. M. Tissue, J. Lumin. 1998, 76&77, 234-237.
[103] R. S. Meltzer, K. S. Hong, Phys. Rev. B: Condens. Matter Mat. Phys. 2000, 61, 3396-3403.

[104] R. S. Meltzer, W. M. Yen, H. Zheng, S. P. Feofilov, M. J. Dejneka, Phys. Rev. B.: Condens. Matter Mat. Phys. 2001, 64, 100201R (4pp).
[105] F. Beaudoux, A. Ferrier, O. Guillot-Noël, T. Chanelière, J.-L. Le Gouët, Ph. Goldner, Opt. Exp. 2011, 19, 15236-15243.
[106] A. Perrot, Ph. Goldner, D. Giaume, M. Lovrić, C. Adriamiadamanana, R. R. Gonçalves, A. Ferrier, Phys. Rev. Lett. 2013, 111, 203601 (5pp).
[107] R. Kolesov, K. Xia, R. Reuter, R. Stöhr, A. Zappe, J. Meijer, P. R. Hemmer, J. Wrachtrup, Nat. Commun. 2012, 3, 1029 (7pp).
[108] T. Utikal, E. Eichhammer, L. Petersen, A. Renn, S. Götzinger, V. Sandoghdar, Nat. Commun. 2014, 5, 3627 (8pp).
[109] K. de Oliveira Lima, R. Roger Gonçalves, D. Giaume, A. Ferrier, Ph. Goldner, J. Lumin. 2015, 168, 276-282.
[110] G. P. Flinn, K. W. Jang, J. Ganem, M. L. Jones, R. S. Meltzer, R. M. Macfarlane, Phys. Rev. B.: Condens. Matter Mat. Phys. 1994, 49, 5821-5827.
[111] J. G. Bartholomew, K. de Oliveira Lima, A. Ferrier, Ph. Goldner, Nano Lett. 2017, 17, 778-787.
[112] R. M. Macfarlane, R. M. Shelby, J. Lumin. 1987, 36, 179-207.
[113] R. M. Macfarlane, Y. Sun, R. L. Cone, C. W. Thiel, R. W. Equall, J. Lumin. 2004, 107, 310-313.
[114] K. W. Jang, R. S. Meltzer, Phys. Rev. B: Condens. Matter Mat. Phys. 1995, 52, 6431-6439.
[115] T. Lutz, L. Vessier, C. W. Thiel, R. L. Cone, P. E. Barclay, W. Tittel, Phys. Rev. A: At., Mol., Opt. Phys. 2016, 94, 013801 (5pp).
[116] T. Böttger, C. W. Thiel, Y. Sun, R. L. Cone, Phys. Rev. B: Condens. Matter Mat. Phys. 2006, 73, 075101 (16pp).
[117] Y. Sun, C. W. Thirl, R. L. Cone, Phys. Rev. B: Condens. Matter Mat. Phys. 2012, 85, 165106 (13 pp).
[118] T. Lutz, L. Veissier, C. W. Thiel, P. J. T. Woodburn, R. L. Cone, P. E Barclay, W. Tittel, J. Lumin. 2017, 191, 2-12.
[119] T. Lutz, L. Veissier, C. W. Thiel, P. J. T. Woodburn, R. L. Cone, P. E. Barclay, W. Tittel, Sci. Techn. Adv. Mat. 2016, 17, 63-70.
[120] A. Ferrier, C. W. Thiel, B. Tumino, M. O. Ramirez, L. E. Bausa, R. L. Cone, A. Ikesue, Ph. Goldner, Phys. Rev. B: Condens. Matter Mat. Phys. 2014, 87, 041102 (4pp).
[121] N. Kunkel, A. Ferrier, C. W. Thiel, M. O. Ramírez, L. E. Bausá, R. L. Cone, A. Ikesue, Ph. Goldner, APL Mat. 2015, 3, 096103 (6pp).
[122] N. Kunkel, J. Bartholomew, S. Welinski, A. Ferrier, A. Ikesue, Ph. Goldner, Phys. Rev. B: Condens. Matter Mat. Phys. 2016, 94, 184301 (9pp).
[123] A. Ikesue, Y. L. Aung, Nature Phot. 2008, 2, 721-727.
[124] H. Zhang, J. Yang, S. Gray, J. A. Brown, T. D. Ketcham, D. E. Baker, A. Carapella, R. W. Davis, J. G. Arroyo, D. A. Nolan, ACS Omega, 2017, 2, 3739-3744.